Phys. Status Solidi A **208**, No. 8, 1804–1807 (2011) / **DOI** 10.1002/pssa.201001117

physica status solidi a
www.pss-a.com
applications and materials science

Studies of lithium argyrodite solid electrolytes for all-solid-state batteries

R. P. Rao* **and S. Adams****

Department of Materials Science and Engineering, National University of Singapore, 5 Engineering Drive 2, Singapore 117576, Singapore

Received 29 September 2010, revised 3 January 2011, accepted 4 January 2011
Published online 4 July 2011

Keywords argyrodite, bond valence, ionic conductivity, solid electrolytes

* Corresponding author: e-mail mserpr@nus.edu.sg, Phone: +65 6516 7898, Fax: +65 6776 3604
** e-mail mseasn@nus.edu.sg, Phone: +65 6516 6869, Fax: +65 6776 3604

Rechargeable all-solid-state lithium Li-ion batteries (AS-LIBs) are attractive power sources for electrochemical applications; due to their potentiality in improving safety and stability over conventional batteries with liquid electrolytes. AS-LIBs require a Li-fast ion conductor (FIC) as the solid electrolyte. Finding a solid electrolyte with high ionic conductivity and compatibility with other battery components is a key factor in building high performance AS-LIBs. There have been numerous studies, e.g., on lithium rich sulfide glasses as solid electrolytes. However, the limited current density remains a major obstacle in developing competitive batteries based on the known solid electrolytes. Here we prepare argyrodite-type Li_6PS_5X (X = Cl, Br, I) using mechanical milling followed by annealing. XRD characterization reveals the formation and growth of Li_6PS_5X crystals in samples under varying annealing conditions. For Li_6PS_5Cl an ionic conductivity of the order of 10^{-4} S/cm is reached at room temperature, which is close to the Li mobility in conventional liquid electrolytes ($LiPF_6$ in various carbonates) and well suitable for AS-LIBs.

1 Introduction Rechargeable all-solid-state lithium or Li-ion batteries (AS-LIBs) are attractive power sources for applications like "smart" credit cards and medical implants. They need a Li-fast ion conductor (FIC) as the solid electrolyte. The purpose is to improve safety and stability over conventional batteries with liquid electrolyte. Finding a suitable solid electrolyte with high ionic conductivity is a pivotal issue for building practical solid-state batteries. There have been numerous developments on materials such as lithium rich sulfide glasses as solid electrolyte. However, limited current density remains a major impediment in these electrolyte systems.

Argyrodites form a class of chalcogenide structures related to the mineral Ag_8GeS_6, which includes various fast Ag^+ or Cu^+ ion conductors such as A_7PS_5X ($A = Ag^+, Cu^+$) [1]. Recently, Deiseroth et al. [2] could synthesize the analogue cubic Li^+ argyrodytes with formula Li_6PS_5X (X = Cl, Br, I) and Li_7PS_6. ^{7}Li-NMR relaxation and impedance experiments find an intrinsic local lithium mobility of the Li-argyrodite crystals as high as 10^{-2}–10^{-3} S/cm at room temperature close to the mobility in liquid electrolytes comprising of $LiPF_6$ salt in various carbonates. With such high lithium mobilities, these materials may be ideal for use as solid electrolytes in lithium ion batteries. Here we prepare the argyrodite-type Li_6PS_5X (X = Cl, Br) using mechanical milling followed by annealing of the samples. XRD and impedance measurements of the samples are reported here.

Ion transport studies for the silver and copper thiophosphates can be based on the detailed available anharmonic structure refinements; no comparably detailed studies are so far available for the Lithium compounds due to the low scattering power of Li and phase transitions preventing low-temperature single crystal studies. Therefore we analyze the ion transport pathways in the Li_6PS_5X (X = Cl, Br) phases using optimized empirical force-fields in combination with the bond valence analysis of energy landscapes for the mobile Li^+.

2 Experimental method Li_6PS_5X (X = Cl, Br, I) samples were prepared by high energy mechanical milling using Agate (45 ml pot and 15 number of 10 mm ø ball) pot and balls; Li_2S, P_2S_5, and LiX (X = Cl, Br, I) crystalline powders were used as starting materials. The samples were

ground for 20 h followed by annealing at 550 °C for 5 h. Samples were pressed into 10 mm diameter pellets of ~1.5 mm thick for annealing the samples. All the procedure was done under Ar atmosphere. The annealed samples were characterized by X-ray powder diffractometry using Cu Kα radiation (PANalytical X'Pert PRO) equipped with a fast linear detector. XRD data were collected in the $2\theta^\circ$ range 8–100° with a nominal scan rate of 120 s step-1 and a step size of 0.016° at room temperature. Rietveld refinements of XRD powder patterns were performed with the generalized structure analysis system (GSAS) by Larson and von Dreele [3], along with the graphical user interface EXGUI [4]. Structure data from published from single crystal X-ray data measurements by Deiseroth et al. [2]. The structures were thus refined based on the same set of 49 refinable parameters: 12 background variables of shifted Chebyshev function, 7 profile variables, 1 cell parameter, 24 refinable atomic coordinates, 3 atomic displacement parameters, 1 preferential orientation parameter and an overall scale factor. Ionic conductivity measurements of ball milled and final samples at different temperatures were carried out by impedance spectroscopy (Schlumberger Solartron SI1260) in the frequency range of 1 Hz to 10 MHz. Stainless steel plates were used as electrodes. At each temperature the samples were kept for 20 min for thermal equilibration. The bulk resistance R_b was determined from fitting impedance data to Nyquist plots. The equivalent circuit consists of C_b, R_b, and a Warburg element.

3 Bond valence approach Empirical relationships between bond length R and bond valence S are widely used in crystal chemistry to identify plausible equilibrium sites for an atom in a structure as sites where the BV sum of the atom matches its oxidation state,

$$S_{\text{Li-X}} = \exp\left[\frac{(R_0 - R)}{b}\right]. \quad (1)$$

A systematic adjustment of BV parameters b to the bond softness, together with the inclusion of interactions beyond the first coordination shell permits more adequate estimates of non-equilibrium site bond valences. The modeling of pathways for mobile Li^+ as regions of low site energy E(Li) (or of low bond valence sum mismatch $|\Delta V(\text{Li})|$) has been demonstrated to be a simple and reliable way of identifying transport pathways in local structure models, provided that the local structure model captures the essential structural features. While bond valences $s_{\text{Li-S}} = \exp[(R_0 - R_{\text{Li-S}})/b]$ and hence the BV sum mismatch $|\Delta V|$ are mostly expressed in arbitrary "valence units," they may – as we have shown recently [5–11] – also be linked to an absolute energy scale by expressing the bond valence as a Morse-type interaction energy:

$$E = D_0\left\{\left[\frac{(s - s_{\min})^2}{s_{\min}^2}\right]^{-1}\right\} = D_0\left\{s_{\text{rel}}^2 - 2s_{\text{rel}}\right\}. \quad (2)$$

Here, s_{rel} equals $s/s_{\min}$ and $s_{\min}$ represents the value of the bond valence for the equilibrium distance $R_{\min}$, which is estimated from the bond valence parameter R_0 and typical coordination number NC of the cation (for details see Ref. [9]). Pathways for Li^+ can then be modeled as regions in the structure as described in our previous reports [10]. These pathways are visualized as regions enclosed by isosurfaces of constant E(Li) based on a grid of E(Li) values with a resolution <0.1 Å covering the unit cell. The threshold value of E(Li) for which the E(Li) isosurfaces form a continuous migration pathway (that includes both occupied and vacant Li sites), permits a rough estimate of the activation energy for the Li+ ion transport process. As such an approach neglects relaxation, the assessment of the activation energy is based on an empirical correlation observed for a wide range of Lithium ion conductors.

4 Results and discussion The XRD patterns of ball milled samples showed partial crystallinity with peaks belonging to the Li_2S, P_2S_5, and LiX (X = Cl, Br, I) phases. While for the samples that have been ball-milled for 24 h, peaks of various phases are still rather prominent; peaks of most phases except Li_2S become very broad after 24 h. After annealing both samples yield the respective argyrodite phases with comparable crystallinity. Thus preparation time for argyrodites could be drastically reduced when compared to the original synthesis recipe [2], where the preparation takes 7 days. Figure 1 shows the Rietveld fit to the final Li_6PS_5I system.

The final samples of Li_6PS_5Cl, Li_6PS_5Br, and Li_6PS_5I exhibit the high symmetry aristotype of the argyrodite structure in space group F-43m (see Fig. 1). The lattice parameters of Li_6PS_5Cl, Li_6PS_5Br, and Li_6PS_5I are 9.850(4), 9.980(8) and 10.142(3) Å, respectively. These values are in good agreement with the reported values. SEM images of both samples showed the formation of about 100 nm nano crystals for Li_6PS_5Br. SEM of the ball milled sample before

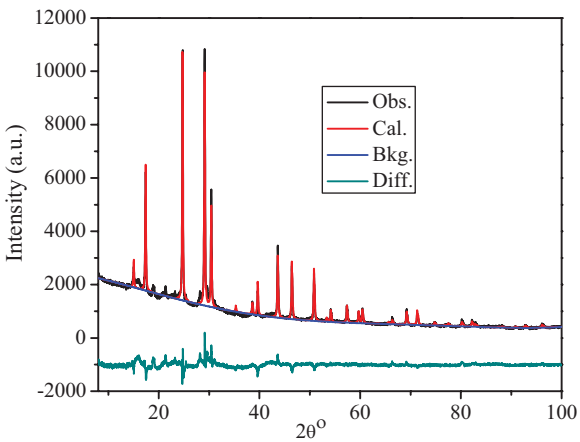

Figure 1 (online color at: www.pss-a.com) Rietveld refinement of crystalline Li_6PS_5I.

annealing showed the partially crystalline nature of the compound. Temperature dependent ionic conductivity of both samples as determined from impedance spectra showed Arrhenius nature. Ball milled Li_6PS_5Cl, Li_6PS_5Br, and Li_6PS_5I samples have exhibit ionic conductivity 3.3×10^{-5}, 3.2×10^{-5}, and 2.2×10^{-4} S/cm with activation energies 0.38, 0.32, and 0.26 eV, respectively. The ionic conductivities of final crystalline compounds are 1.9×10^{-3}, 6.8×10^{-3}, and 4.6×10^{-7} S/cm, respectively. Low temperature ionic conductivity studies to determine the activation energy of the crystalline compounds are in progress in our laboratory.

Figure 2 compares Li^+ ion migration pathways in the Li_6PS_5X argyrodite structures with X = Cl, Br, and I.

Roughly speaking, the three-dimensional pathway network for long range (dc) ion conduction in all Li_6PS_5X phases consist of interconnected low-energy local pathway cages.

In detail however these cages and the way in which they are interconnected differs for the compounds with different

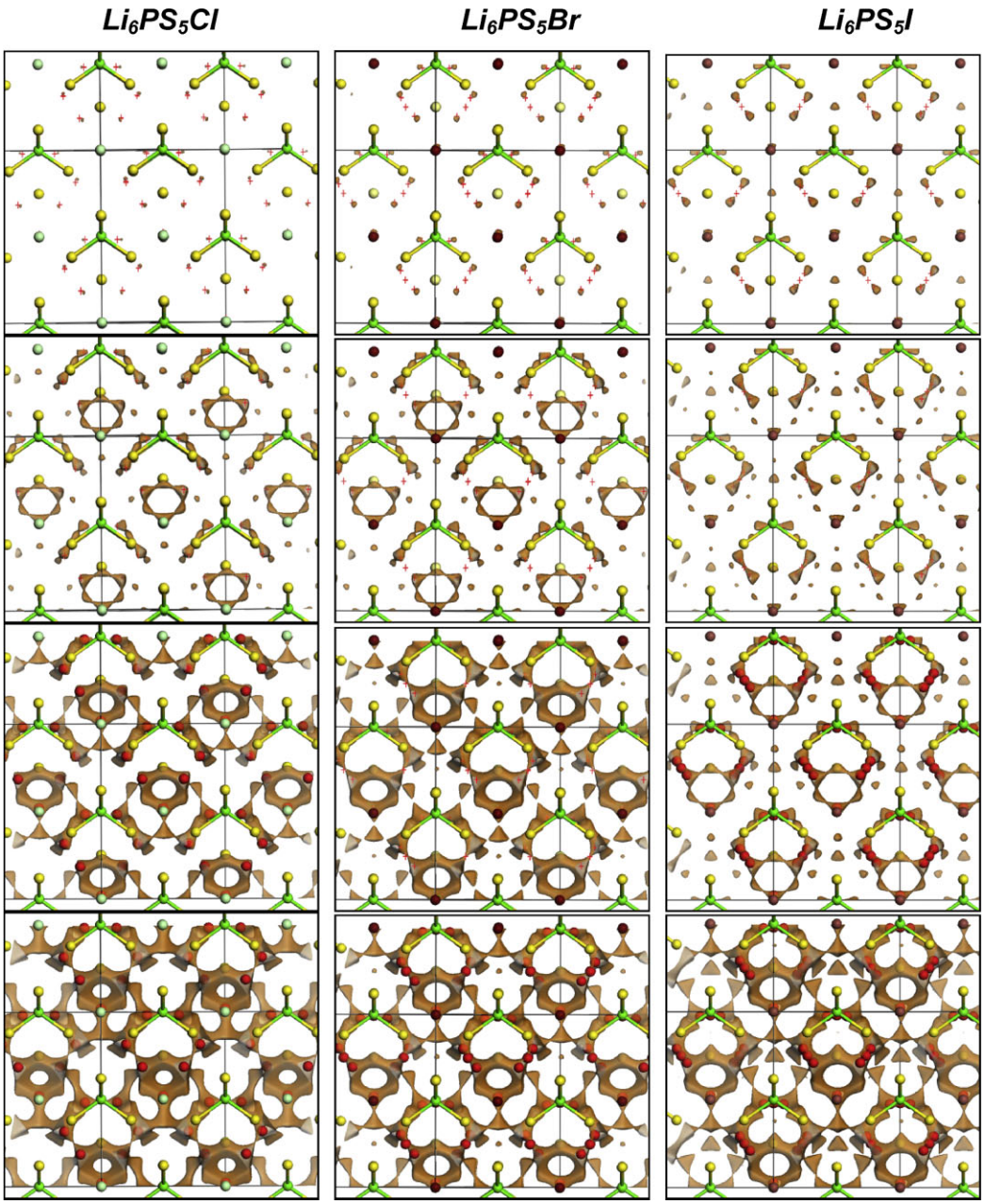

Figure 2 (online color at: www.pss-a.com) Li^+ migration pathways of Li_6PS_5X (X = Cl, Br, I; left to right) for different energy thresholds characterizing equilibrium sites (1st row), first local Li^+ paths (2nd row), extended local Li^+ pathway cages (3rd row), and pathways for long range Li^+ migration. Note that pathways are different in detail (cf. text).

halide ions. In the structure of Li_6PS_5Cl structure (l.h.s. column in Fig. 2) the sites of lowest energy agree with the experimentally refined half-occupied Li1 positions. The lowest energy short range pathway then interconnects three such partially occupied Li sites via three interstitial sites forming a pathway hexagon ($E_A = 0.18$ eV). Four such hexagons are then interconnected at a slightly higher energy threshold via a second interstitial site to form an extended pathway cage around the nominal Cl position ($E_A = 0.22$ eV) and the 3D long range pathway network is finally established by a direct connection in-between the cages ($E_A = 0.35$ eV).

For the case of Li_6PS_5I however, experimental studies suggest a more disordered Li distribution described in Ref. [2] by Li1–Li2–Li1 triplet sites. In our bond valence model the sites of lowest E(Li) accordingly imply a disordered Li distribution over the Li1 sites only. The lowest energy interconnection between sites then includes the Li2 site in-between pairs of Li1 sites (0.09 eV), but the Li2 position appears not to be a local minimum of E(Li), which is also in line with the difference Fourier plot shown in Ref. [11]. Experimental NMR data find an even lower activation energy of 0.043 eV for unspecified local hops [2]. Six of these dumbbell-like local pathways (which correspond to the intercage pathways in Li_6PS_5I) then form a pathway cage around the S2 site (not as in the previous case around the halide ion) with $E_A = 0.15$ eV. The cages are finally interconnected via an interstitial site for $E_A = 0.33$ eV in remarkable agreement with the experimental value 0.32 eV from low temperature impedance spectroscopy and 0.30 eV from MD simulations. MD simulations also suggest 0.14 eV for a localized motion. [11].

The characteristics of Li^+ pathways in Li_6PS_5Br appear to mix features of pathways in the cases X = Cl and X = I cases. Again, there is a clear disorder over Li1 sites (The experimental structure determination again suggests a Li1-Li2-Li1 triplet). The lowest energy local pathway interconnecting these sites is a hexagon of three Li1 and three interstitial sites as in Li_6PS_5Cl ($E_A = 0.15$ eV). The local pathway cage forms as in Li_6PS_5I around the S2 site (the site is effectively occupied by 84% S/16% Br according to Ref. [11]) for $E_A = 0.25$ eV, but only at a minutely lower energy than for the long range pathways ($E_A = 0.27$ eV), which may be thought of as a combination of cages around S2 and around the halide site (which again is occupied by a mixture of Br and S). Preliminary neutron data point toward a similar anion disorder for Li_6PS_5Cl. It should also be kept in mind that the bond valence model of Li_6PS_5Br may be less accurate, as it is based on the experimental structure determination of a crystal that had a slightly lower Br content and a disorder of S and Br over the S2/Br2 and Br3/S3 sites.

It might be noteworthy that analogous oxide argyrodites Li_6PO_5X (X = Cl, Br) have also been reported recently [12]. Due to the different position of oxide ion O2 in these from the S2 position in Li_6PS_5X, pathway cages, and long range pathways found for the oxide argyrodites differ fundamentally. From the significantly higher activation energies found in bond valence models for local (0.4 eV) and long range pathways (0.57 eV) in Li_6PO_5Cl, and the absence of interstitial sites in these pathways it can be understood why the oxide analogues show an oders of magnitude lower conductivity ($\sim 10^{-9}$ S/cm at ambient temperature, experimental activation energy 0.66 eV).

5 Conclusions Li_6PS_5X (X = Cl, Br) argyrodite structures were prepared by mechanical milling followed by annealing of the samples. This allows for a faster synthesis than the earlier reported long annealing. The obtained crystalline phase showed ionic conductivity of the order of 10^{-3} S/cm at ambient temperature for argyrodites exhibiting anion disorder (X = Cl, Br). Bond valence based Li^+ ion migration pathways for both compounds yield pathways with similarly low activation energies for long range transport (ca. 0.3 eV), despite the pronounced differences in the pathway topology for different halide ions. It could be clarified that the even lower activation energies reported from NMR studies refer to hops within extended local pathway cages that are not directly relevant for the dc conductivity. Due to the high ionic conductivity of the compounds at room temperature, these compounds are of high technological interest as one of the best solid electrolytes for high energy all solid state battery applications.

Acknowledgements Financial support to S. A. in the frame of the Singapore Ministry of Education grant MOE2009-T2-1-065 is gratefully acknowledged.

References

[1] R. B. Beeken, J. J. Garbe, J. M. Gillis, N. R. Petersen, B. W. Podoll, and M. R. Stoneman, J. Phys. Chem. Solids **66**, 882 (2005).
[2] H.-J. Deiseroth, S.-T. Kong, H. Eckert, J. Vannahme, C. Reiner, T. Zaiß, and M. Schlosser, Angew. Chem. **120**, 767 (2008).
[3] A. C. Larson and R. B. von Dreele, General Structure Analysis System (GSAS); Report LAUR 86-748; Los Alamos National Laboratory, Los Alamos, NM (2000).
[4] B. J. Toby, J. Appl. Crystallogr. **34**, 210 (2001).
[5] S. Adams, J. Power Sources **159**, 200 (2000).
[6] S. Adams, Acta Crystallogr. B Struct. Sci. **57**, 278 (2001).
[7] S. Adams and J. Swenson, Solid State Ionics **175**, 665 (2004).
[8] S. Adams, Solid State Ionics **177**, 1625 (2006).
[9] S. Adams and R. Prasada Rao, Phys. Chem. Chem. Phys. **11**, 3210 (2009).
[10] R. P. Rao, T. D. Tho, and S. Adams, Solid State Ionics **181**, 1 (2010).
[11] O. Pecher, S.-T. Kong, T. Goebel, V. Nickel, K. Weichert, Ch. Reiner, H.-J. Deiseroth, J. Maier, F. Haarmann, and D. Zahn, Chem. Eur. J. **16**, 8347 (2010).
[12] S.-T. Kong, H.-J. Deiseroth, J. Maier, V. Nickel, K. Weichert, and C. Reiner, Z. Anorg. Allg. Chem. **636**, 1920 (2010).